A Numerical Analysis on the Ionized Boundary Layer along a Shock Tube Side Wall

AUTHOR(S):

TAKANO, Yasunari; AKAMATSU, Teruaki

CITATION:

TAKANO, Yasunari ...[et al]. A Numerical Analysis on the Ionized Boundary Layer along a Shock Tube Side Wall. Memoirs of the Faculty of Engineering, Kyoto University 1975, 36(4): 333-347

ISSUE DATE:

1975-03-25

URL:

http://hdl.handle.net/2433/280955

A Numerical Analysis on the Ionized Boundary Layer along a Shock Tube Side Wall

By

Yasunari TAKANO* and Teruaki AKAMATSU**

(Received June 12, 1974)

Abstract

A numerical analysis was made for the ionized reacting, thermal non-equilibrium boundary layer which develops along a shock-tube side-wall, behind an ionizing incident shock wave. The boundary layer was found to change according to the ionization relaxation of the inviscid flow behind the shock wave. It was shown that the temperature in the boundary layer becomes higher than the temperature outside of the boundary layer in the rapidly ionizing region behind the shock wave.

The numerical solutions were obtained for the case of the incident shock Mach number $M_S=13$, initial pressure $p_1=10$ torr and initial temperature $T_1=300°K$.

Nomenclature

C : degree of ionization
C_p : specific heat
D_a : ambipolar diffusion coefficient
f : non-dimensional stream function
h : enthalpy
k : Boltzmann constant
k_{fa} : ionization reaction rate coefficient by atom-atom inelastic collisions
k_{fe} : ionization reaction rate coefficient by atom-electron inelastic collisions
k_{re} : three body recombination rate coefficient
m : dimensionless degree of ionization C/C_δ
m_a : mass of a heavy particle
m_e : mass of an electron
M_s : incident shock Mach number
n_a : number density of atoms

* Former graduate student, now studying at the Department of Mechanical Engineering as a research student.
** Department of Mechanical Engineering

n_e : number density of electrons
p : pressure
P_r : Prandtl number
R : energy transfered from heavy particles to electrons due to elastic collisions
R_A : gas constant
S_c : Schmidt number
T : temperature of heavy particle gas
T_e : temperature of electron gas
T_{A1} : characteristic temperature for excitation
T_{ion} : characteristic temperature for ionization
u : velocity, dimensionless velocity u/u_δ
U_s : incident shock speed
x : coordinate
y : coordinate
η : non-dimensional coordinate
θ : dimensionless temperature of heavy particle gas T/T_δ
Θ : dimensionless temperature of electron gas $T_e/T_{e\delta}$
λ : thermal conductivity of heavy particle gas
λ_e : thermal conductivity of electron gas
μ : viscosity
ν_e : collision frequency for electrons and heavy particles
ξ : non-dimensional coordinate
ρ : density

Introduction

Flush-mounted electrodes on a shock-tube side-wall are widely used to measure an ionized gas behind an incident shock wave. The success of these measurements depends on the understanding of an ionization relaxation behind a shock wave and a boundary layer along a shock-tube side-wall. The free-stream behind a shock wave is ionized reacting. In a state of thermal non-equilibrium, it changes in velocity, temperature and degree of ionization. Therefore, the solutions of the boundary layer equations are not similar.

The present work concerns a numerical analysis about an ionized reacting and thermally non-equilibrium boundary layer which develops along a shock-tube side-wall, behind an incident ionzing shock wave. It can bring light on such problems that boundary layers vary according to sudden changes of the free-stream on the outer edge of boundary layers.

Knöös[1] and Honma & Aoki[2] studied the problems of shock-tube side-wall boundary layers. Their analyses are based on the assumptions that the free-stream is equilibrium, and the boundary layer is equilibrium or quasi-equilibrium. Analyses of flat plate boundary layers in partially ionized gases, which are obtained in a low density plasma wind tunnel, were carried out by Tseng & Talbot[3] considering thermal non-equilibrium and recombination, and also by Matsuoka & Nishida[4] considering thermal non-equilibrium. A detailed review of numerical analyses for boundary layer equations was made by Blottner[5]. Recently, Chung, Talbot & Touryan[6] summarized and discussed the theoretical results on electric probes.

We will obtain numerical solutions of the boundary layer over a shock-tube side-wall for the case where an incident shock wave, whose shock Mach number is $Ms=13$, propagates into a stationary argon gas of initial pressure $p_1=10$ torr and initial temperature $T_1=300°K$. This condition can be produced by the free-piston shock tube in our laboratory.

2. Ionization Relaxation behind an Incident Shock Wave

Several authors[7),8)] analyzed problems of a relaxation zone behind an ionizing shock wave which propagates into a stationary argon gas. In this study, we will carry out calculations by using the method of Hoffert & Lien[7]. In a coordinate travelling at the velocity U_s of the shock front, equations of continuity, momentum, energy, electron number density and electron temperature are

$$\rho u = \rho_1 U_s \tag{1}$$

$$p+\rho u^2 = p_1+\rho_1 U_s^2 \tag{2}$$

$$h+u^2/2 = h_1+U_s^2/2 \tag{3}$$

$$d(n_e u)/dx = \dot{n}_e \tag{4}$$

$$\frac{3}{2} k n_e u \frac{dT_e}{dx} = R-(\dot{n}_e)_e k T_{ion} \tag{5}$$

where $p = \rho R_A(T+CT_e)$

$h = C_p(T+CT_e)+CR_A T_{ion}$

$n_e = \rho C/m_a$

The subscript 1 refers to upstream conditions. The energy transfer rate due to elastic collisions can be written as follows:

$$R = 3n_e(m_e/m_a)k(T-T_e)\nu_e \tag{6}$$

The net rate of electron production $\dot{n}_e$ consists of two processes. One is the reaction rate by atom-atom inelastic collisions;

$$(\dot{n}_e)_a = k_{fa}(T)n_a^2 \tag{7}$$

The other is the reaction by atom-electron inelastic collisions and three body recombination rate:

$$(\dot{n}_e)_e = k_{fe}(T_e)n_a n_e - k_{re}(T_e)n_e^3 \tag{8}$$

Therefore, the net rate of electron production $\dot{n}_e$ is written as follows:

$$\dot{n}_e = (\dot{n}_e)_a + (\dot{n}_e)_e \tag{9}$$

In the present work, we assume that the electron temperature is in a local steady state: the left hand side term of eq. (5) is everywhere much smaller than either of the terms on the right hand side. Thus, the following equation is used instead of eq. (5).

$$T - T_e = \frac{1}{3}\frac{m_a}{m_e}\frac{(\dot{n}_e)_e}{n_e \nu_e} T_{ion} \tag{10}$$

We carry out numerical calculations at a shock Mach number $Ms=13$, upsteam pressure $p_1=10$ torr and upstream temperature $T_1=300°K$. Fig. 1 shows variables of flow properties in a relaxation region, normalyzed by the equilibrium zone. The flow properties at the equilibrium zone are

$$u_0 = 748\ m/s\,, \quad T_0 = 11762°K\,, \quad C_0 = 0.058$$
$$\rho_0 = 1.20\times 10^4\ \mathrm{g/cm^3}\,, \quad n_{e0} = 1.04\times 10^{17}\ \mathrm{cm^{-3}}$$

A characteristic length l of the ionization reaction in the equilibrium zone is taken as a unit length of the coordinate. At present, $l=0.68$ cm.

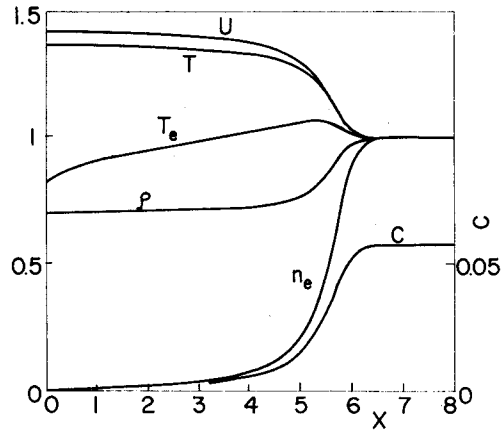

Fig. 1. Variation of flow properties in the ionization relaxation region behind an incident shock wave.

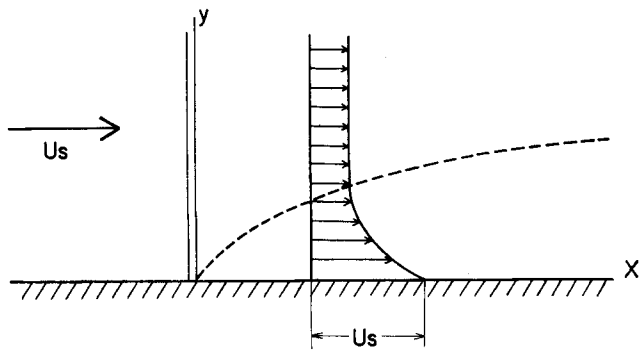

Fig. 2. Boundary layer along a shock-tube side-wall.

3. Boundary Layer over a Shock-Tube Side-Wall

The numerical analysis for an ionized boundary layer along a shock-tube side-wall is made with the following assumptions: (i) the ionization relaxation to equilibrium occurs in the freestream behind a shock wave; (ii) ions and electrons are ambipolar; (iii) the electron gas is in a state of thermal non-equilibrium with the heavy particle gas; (iv) the electron production rate consists of atom-atom ionization rate, atom-electron ionization rate and three body recombination rate; (v) the velocity on the wall is U_s and the temperature of heavy particles on the wall is equal to the wall temperature T_w; (vi) the wall potential is floating; (vii) the wall surface is a catalytic metal; (viii) the boundary conditions of the ionization degree and the electron temperature on the wall are derived from the assumption of a free fall sheath.

Basic equations are steady two-dimensional boundary layer equations. Let x and y be coordinates along the wall measured from the wave front and one perpendicular to the wall, respectively. The equations of continuity, momentum, energy, ionization degree and electron temperature are

$$\frac{\partial(\rho u)}{\partial x}+\frac{\partial(\rho v)}{\partial y}=0 \tag{11}$$

$$\rho\left(u\frac{\partial u}{\partial x}+v\frac{\partial u}{\partial y}\right)=-\frac{dp}{dx}+\frac{\partial}{\partial y}\left(\mu\frac{\partial u}{\partial y}\right) \tag{12}$$

$$\rho\left(u\frac{\partial H}{\partial x}+v\frac{\partial H}{\partial y}\right)=-\frac{\partial q}{\partial y}+\frac{\partial}{\partial y}\left(u\mu\frac{\partial u}{\partial y}\right) \tag{13}$$

$$\rho\left(u\frac{\partial C}{\partial x}+v\frac{\partial C}{\partial y}\right)=\frac{\partial}{\partial y}\left\{\rho D_a\frac{\partial}{\partial y}\left(C\frac{1+T_e/T}{2}\right)\right\}+m_a\dot{n}_e \tag{14}$$

$$\rho C_p\left\{u\frac{\partial(CT_e)}{\partial x}+v\frac{\partial(CT_e)}{\partial y}\right\}$$
$$=\frac{\partial}{\partial y}\left\{\lambda_e\frac{\partial T_e}{\partial y}+C_pT_e\rho D_a\frac{\partial}{\partial y}\left(C\frac{1+T_e/T}{2}\right)\right\}+R-kT_{ion}(\dot{n}_e)_e \tag{15}$$

where $H=C_p(T+CT_e)+CR_AT_{ion}+u^2/2$

$$q=-\lambda\frac{\partial T}{\partial y}-\lambda_e\frac{\partial T_e}{\partial y}-(R_AT_{ion}+C_pT_e)\rho D_a\frac{\partial}{\partial y}\left(C\frac{1+T_e/T}{2}\right)$$

In the electron temperature equation (15), the term $v\nabla p_e$ is dismissed. This term is very small compared with others on the right hand side of eq. (15). Chung & Mullen[9] also disimissed this term in their study on non-equilibrium electron temperature. This dismissal makes the analyses somewhat easier. Temperature equation of heavy particles can be obtained from eqs. (12), (13) and (14).

$$\rho C_p\left(u\frac{\partial T}{\partial x}+v\frac{\partial T}{\partial y}\right)-u\frac{dp}{dx}=\frac{\partial}{\partial y}\left(\lambda\frac{\partial T}{\partial y}\right)+\mu\left(\frac{\partial u}{\partial y}\right)^2-R-kT_{ion}(\dot{n}_e)_a \tag{16}$$

Eqs. (14) and (15) reduce to

$$\rho C_pC\left(u\frac{\partial T_e}{\partial x}+v\frac{\partial T_e}{\partial y}\right)=\frac{\partial}{\partial y}\left(\lambda_e\frac{\partial T_e}{\partial y}\right)+\rho D_a\frac{\partial}{\partial y}\left(C\frac{1+T_e/T}{2}\right)\frac{\partial}{\partial y}(C_pT_e)$$
$$+R-\{(kT_{ion}+m_aC_pT_e)(\dot{n}_e)_e+m_aC_pT_e(\dot{n}_e)_a\} \tag{17}$$

The electron production due to atom-atom inelastic collisions is not so important as that due to atom-electron collisions except in the initial stage of ionization. Moreover, the kinetic energy of electrons produced by atom-atom inelastic collisions is still not clear. Hence, the terms containing $(\dot{n}_e)_a$ in eqs. (16) and (17) are omitted. It is worth noting that the term of $(\dot{n}_e)_a$ in eq. (14) can not be omitted because of compatibility with the conditions at the boundary layer edge.

Boundary conditions for eqs. (11)–(17) are

$$y=0;\quad u=U_s,\quad v=0,\quad T=T_w \tag{18}$$

$$y\to\infty;\quad u\to u_\delta(x),\quad C\to C_\delta(x),\quad T\to T_\delta(x),\quad T_e\to T_{e\delta}(x) \tag{19}$$

where subscript δ refers to the boundary layer edge.

4. Boundary Layer Equations

Chung[10] reviewed the boundary layer theory of chemical reacting dissociative gas, which is available in analyzing the present problem of an ionizing boundary layer.

4.1 Transformations

The following similar transformations are introduced:

$$\xi = \int_0^x (\rho\mu)_\delta u_\delta dx\,, \quad \eta = \frac{u_\delta}{\sqrt{2\xi}} \int \rho dy$$

New variables are defined as follows:

$$f = u/u_\delta\,, \quad m = C/C_\delta\,, \quad \theta = T/T_\delta\,, \quad \Theta = T_e/T_{e\delta}$$

With the assumptions that $\rho\mu$, P_r and S_c are constants, eqs. (12), (14), (16) and (17) are reduced to

$$2\xi(f_\eta f_{\xi\eta} - f_\xi f_{\eta\eta}) = f_{\eta\eta\eta} + f f_{\eta\eta} + (2\xi/u_\delta)(du_\delta/d\xi)(\theta - f_\eta^2) \tag{20}$$

$$2\xi(f_\eta m_\xi - f_\xi m_\eta) = M_{\eta\eta}/S_c + f m_\eta - (2\xi/C_\delta)(dC_\delta/d\xi) m f_\eta + \zeta_a\phi_a + \zeta_f\phi_f - \zeta_r\phi_r \tag{21}$$

$$2\xi(f_\eta\theta_\xi - f_\xi\theta_\eta) = \theta_{\eta\eta}/P_r + f\theta_\eta + (u_\delta^2/C_p T_\delta) f_{\eta\eta}^2 - \sigma C_\delta \tau R - (2\xi/C_p T_\delta) d(C_p T_\delta + u_\delta^2/2)/d\xi \cdot \theta f_\eta \tag{22}$$

$$2\xi(f_\eta\Theta_\xi - f_\xi\Theta_\eta) = \frac{1}{P_{re}}\frac{1}{m}(\kappa\Theta_\eta)_\eta + \frac{1}{S_c}\frac{M_\eta\Theta_\eta}{m} + f\Theta_\eta - \frac{2\xi}{T_{e\delta}}\frac{dT_{e\delta}}{d\xi}\Theta f_\eta + \sigma\frac{R}{m} - \left(\frac{R_A T_{ion}}{C_p T_{e\delta}} + \Theta\right)\frac{\zeta_f\phi_f - \zeta_r\phi_r}{m} \tag{23}$$

where $M = \dfrac{m}{2}\left(1 + \tau\dfrac{\Theta}{\theta}\right)$ $\quad R = \left(\dfrac{\theta}{\tau} - \Theta\right)\dfrac{m^2}{\Theta^{3/2}}$

$$\kappa = \frac{\Theta^{5/2}}{\theta} \quad \tau = \frac{T_{e\delta}}{T_\delta} \quad P_{re} = P_r\frac{C_\delta\lambda_\delta}{\lambda_{e\delta}}$$

$$\phi_a = \theta^{1/2}\frac{1/\theta + 2T_\delta/T_{A1}}{1 + 2T_\delta/T_{A1}} \exp\left\{\frac{T_{A1}}{T_\delta}\left(1 - \frac{1}{\theta}\right)\right\}$$

$$\phi_f = \frac{\Theta^{3/2}}{\theta}\frac{1/\Theta + 2T_{e\delta}/T_{A1}}{1 + 2T_{e\delta}/T_{A1}} \exp\left\{\frac{T_{A1}}{T_{e\delta}}\left(1 - \frac{1}{\Theta}\right)\right\} m$$

$$\phi_r = \frac{1}{\theta^2}\frac{1/\Theta + 2T_{e\delta}/T_{A1}}{1 + 2T_{e\delta}/T_{A1}} \exp\left\{\frac{T_{ion} - T_{A1}}{T_{e\delta}}\left(\frac{1}{\Theta} - 1\right)\right\} m^3$$

In these reductions of equations, such relations are used that $\rho/\rho_\delta = 1/\theta$ and $\lambda_e/\lambda_{e\delta} = \Theta^{5/2}$. The collision frequency for electrons and heavy particles, which appears in the term of energy transfer due to elastic collisions, is assumed to be the electron-ion collision frequency. Several parameters in the transformed boundary layer equations are written as follows:

$$\zeta_a = \tau_u/\tau_a\,, \quad \zeta_f = \tau_u/\tau_f\,, \quad \zeta_r = \tau_u/\tau_r\,, \quad \sigma = \tau_u/\tau_T$$

where $\tau_u = 2\xi/\{(\rho\mu)_\delta u_\delta^2\}$, $\tau_a = n_{e\delta}/\{k_{fa}(T_\delta)n_{a\delta}^2\}$
$\tau_f = 1/\{k_{fe}(T_{e\delta})n_{a\delta}\}$, $\tau_r = 1/\{k_{re}(T_{e\delta})n_{e\delta}^2\}$
$\tau_T = (6/5)(m_e/m_a)\nu_{e\delta}$

τ_u is a characteristic time of the flow. τ_a, τ_f and τ_r are characteristic times of the atom-atom ionization, the atom-electron ionization and three body recombination, respectively. τ_T is a characteristic time of the energy transfer. Fig. 3 shows parameters obtained from the calculations of ionization relaxation (Fig. 1).

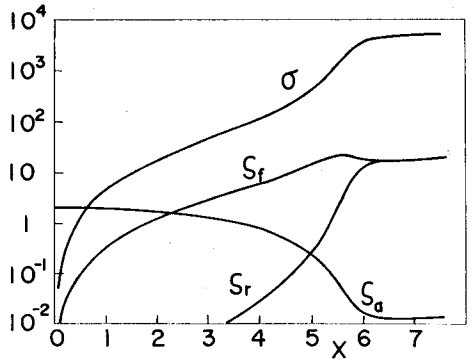

Fig. 3. Variation of parameters of the boundary layer.

4.2 Boundary Conditions and Initial Data

The boundary conditions for transformed boundary layer equations are

$$\eta = 0: f = 0\,, \quad f_\eta = U_s/u_\delta\,, \quad \theta = T_w/T_\delta \tag{24}$$

$$m = 0\,, \quad \Theta_\eta = 0 \tag{25}$$

$$\eta \to \infty: f_\eta,\ m,\ \theta,\ \Theta \to 1 \tag{26}$$

Eqs. (24) and (26) correspond to eqs. (18) and (19). Eq. (25) will be discussed in the Appendix.

At $\xi = 0$, the functions of f, m, θ and Θ must satisfy the equations (20)–(23) whose parameters are

$$\zeta_f = \zeta_r = \sigma = 0$$
$$\zeta_a = (2\xi/C_\delta)(dC_\delta/d\xi) = 2$$
$$(2\xi/u_\delta)(du_\delta/d\xi) = (2\xi/C_pT_\delta)d(C_pT_\delta + u_\delta^2/2)/d\xi$$
$$= (2\xi/T_{e\delta})(dT_{e\delta}/d\xi) = 0$$

The equations (20)–(23) reduce to ordinary differential equations at $\xi = 0$. The solutions of these differential equations, which satisfy the boundary conditions (24)–(26), are taken as initial data. Specially, $\Theta \equiv 1$ at $\xi = 0$.

Parameters which appear in eqs. (20)–(23) must satisfy the following relations because of the compatibility at $\eta \to \infty$.

$$(2\xi/C_\delta)(dC_\delta/d\xi) = \zeta_a+\zeta_f-\zeta_r \tag{27}$$

$$(2\xi/C_pT_\delta)d(C_pT_\delta+u_\delta^2/2)/d\xi = -\sigma C_\delta\tau R_\delta-\zeta_a C_\delta\tau R_A T_{ion}/(C_pT_\delta) \tag{28}$$

$$(2\xi/T_{e\delta})(dT_{e\delta}/d\xi) = \sigma R_\delta-(R_A T_{ion}/C_pT_\delta+1)(\zeta_f-\zeta_r) \tag{29}$$

where $R_\delta = 1/\tau-1$

These equations must satisfy the boundary layer equations at the boundary layer edge. In the present work, the right hand side term of the eqs. (27)—(29) is determined by the values obtained in the analysis of the relaxation region (Fig. 3).

5. Finite Difference Equations

For convenience of a numerical computation, we put $u=f_\eta$, then

$$f_\xi = \int_0^\eta u_\xi d\eta \tag{30}$$

The equation (20) can be written as follows:

$$2\xi(uu_\xi-f_\xi u_\eta) = u_{\eta\eta}+fu_\eta+(2\xi/u_\delta)(du_\delta/d\xi)(\theta-u^2) \tag{31}$$

When we replace the equations (30), (31), (21), (22) and (23) with finite difference equations according to the Crank-Nicolson's method, the resulting difference equations are

$$f_j^{n+1}-f_j^n = h\sum_{i=2}^{j}\left(\frac{u_{i-1}^{n+1}+u_i^{n+1}}{2}-\frac{u_{i-1}^n+u_i^n}{2}\right) \tag{32}$$

$$(\xi^n+\xi^{n+1})\frac{u_j^{n+1}+u_j^n}{2}\frac{w_j^{n+1}-w_j^n}{k}-\frac{f_j^{n+1}-f_j^n}{k}\frac{1}{2}\left(\frac{w_{j+1}^{n+1}-w_{j-1}^{n+1}}{2h}+\frac{w_{j+1}^n-w_{j-1}^n}{2h}\right)$$
$$= (L_{wj}^{n+1}+L_{wj}^n)/2 \tag{33}$$

$$L_{uj}^n = \frac{u_{j+1}^n-2u_j^n+u_{j-1}^n}{h^2}+f_j^n\frac{u_{j+1}^n-u_{j-1}^n}{2h}+X_{u1}^n(\theta_j^n-u_j^{n2}) \tag{34}$$

$$L_{mj}^n = \frac{1}{S_c}\frac{M_{j+1}^n-2M_j^n+M_{j-1}^n}{h^2}+f_j^n\frac{m_{j+1}^n-m_{j-1}^n}{2h}$$
$$-X_c m_j^n u_j^n+\zeta_a^n\phi_{aj}^n+\zeta_r^n\phi_{rj}^n-\zeta_r^n\phi_{rj}^n \tag{35}$$

$$L_{\theta j}^n = \frac{1}{P_r}\frac{\theta_{j+1}^n-2\theta_j^n+\theta_{j-1}^n}{h^2}+f_j^n\frac{\theta_{j+1}^n-\theta_{j-1}^n}{2h}+X_{u2}\left(\frac{u_{j+1}^n-u_{j-1}^n}{2h}\right)^2$$
$$-X_T\theta_j^n u_j^n-\sigma^n C_\delta^n\tau^n R_j^n \tag{36}$$

$$L^n_{\Theta j} = \frac{1}{P_{re}}\frac{\kappa^n_j}{m^n_j}\frac{\Theta^n_{j+1}-2\Theta^n_j+\Theta^n_{j-1}}{h^2}+\frac{1}{P_{re}}\frac{1}{m^n_j}\frac{\kappa^n_{j+1}-\kappa^n_{j-1}}{2h}\frac{\Theta^n_{j+1}-\Theta^n_{j-1}}{2h}$$
$$+\frac{1}{S_c}\frac{1}{m^n_j}\frac{M^n_{j+1}-M^n_{j-1}}{2h}\frac{\Theta^n_{j+1}-\Theta^n_{j-1}}{2h}+f^n_j\frac{\Theta^n_{j+1}-\Theta^n_{j-1}}{2h}$$
$$-X_{Te}\Theta^n_j u^n_j+\sigma^n\frac{R^n_j}{m^n_j}-(E^n_c+\Theta^n_j)\frac{\zeta^n_f\phi^n_{fj}-\zeta_r\phi^n_{rj}}{m^n_j} \tag{37}$$

where subscripts j and n refer to grid points of ξ-direction and η-direction as shown in Fig. 4.

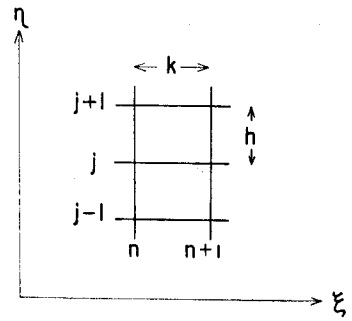

Fig. 4. Grid points of difference schemes.

The boundary conditions for finite difference equations are

$$j=1\ (\eta=0):\ f_1=0\,,\quad u_1=u_w(\xi^n)\,,\quad m_1=0\,,$$
$$\theta_1=\theta_w(\xi^n)\,,\quad \Theta_2=\Theta_1 \tag{38}$$
$$j=N\ (\eta=(N-1)h):\ u_n=m_n=\theta_n=\Theta_n=1 \tag{39}$$

As this system of equations is non-linear, it cannot be solved directly. In order to linearize it, we put $\Delta f_j=f^{n+1}_j-f^n_j$, $\Delta w_j=w^{n+1}_j-w^n_j$ and drop the quadratic terms. The resulting linear system of equations can be written as follows

$$\Delta f_j=(h/2)\sum_{i=2}^{j}(\Delta u_{i+1}+\Delta u_i) \tag{40}$$
$$2(\xi^n+\xi^{n+1})\left(\frac{w^n_{j+1}-w^n_{j-1}}{2h}\frac{\Delta f_j}{k}-u^n_j\frac{\Delta w_j}{k}\right)+\Delta L_{wj}=-2L^n_{wj} \tag{41}$$
$$\Delta L_{wj}=\sum_l\sum_V\left(\frac{\partial L^n_{wj}}{\partial V}\right)\Delta V+\sum_X\left(\frac{\partial L^n_{wj}}{\partial X}\right)\Delta X$$

where $l=j-1, j, j+1$. A function V stands for f, u, m, θ and Θ. A variable X stands for $X_{u_1}, \cdots, X_{Te}, \zeta_a, \cdots, \sigma, \tau, C_\delta, \cdots, T_{e\delta}, \cdots, E_c$, etc. The truncation error of this system is not under the influence of linearization. When f^n_j, u^n_j, m^n_j, and Θ^n_j $(j=1, \cdots, N)$ are known, the unknown variables Δf_j, Δu_j, Δm_j, $\Delta\theta_j$ and $\Delta\Theta_j$ can be obtained by solving the system of $5(N-1)$ simultaneous linear algebraic equations.

6. Result and Discussion

The numerical analysis was made for the case of shock Mach number $M_s=13$ ($U_s=4.2$ Km/s), initial pressure $p_1=10$ torr and initial temperature $T_1=300°K$. In this calculation, similar parameters of $P_r=0.7$, $S_c=2.3$ and $P_{re}=0.0179$ are used. Parameters in the non-dimensional boundary layer equations are obtained from the numerical results in the relaxation region of the free-stream. In the numerical program, 61 points are employed from $\eta=0$ to 6 across the boundary layer with the mesh size $h=0.1$. With the step size along the shock-tube side-wall being $\Delta x=0.01$, the numerical calculation was carried out from $x=0$ to 7.6 for 760 steps.

We made this numerical analysis with the SUBROUTINE GAUELS of the Gauss elimination method, using Kyoto University's Computer FACOM-230-75.

The ionization relaxation region of the free-stream shown in Fig. 1 can be divided into three parts. One is the frozen region from $x=0$ to 4. Another is the region between $x=4$ and 6 where rapid ionization occurs. The other is the equilibrium region of $x\geq 6$. The boundary layer flow was found to vary according to the change of the free-stream.

Fig. 5 shows temperature profiles of heavy particles in the boundary layer.

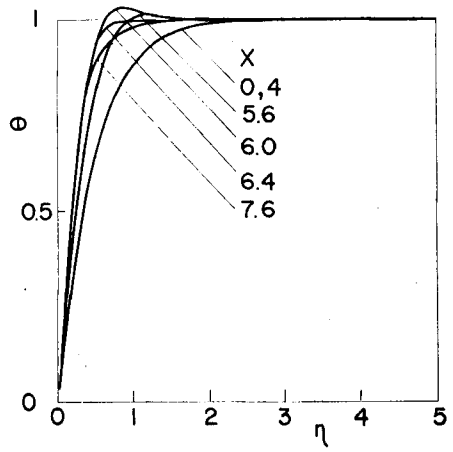

Fig. 5. Temperature profiles of heavy particles in the boundary layer.

The temperature distribution does not vary in the region from $x=0$ to 4. In the region where the rapid ionization occurs and the temperature decreases in the free-stream, it was found that the temperature in the boundary layer becomes higher than that of the free-stream. The reason for this phenomenon will be explained below. The flow patterns of the free-stream and the boundary layer are shown in Fig. 6. Let us imagine that two gas particles go through the position x_1 at the same

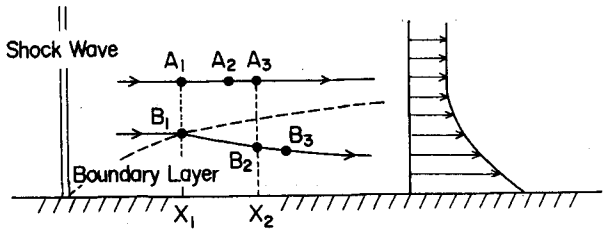

Fig. 6. Flow configuration of a boundary layer.

time. One flows in the free-stream and the other goes into the boundary layer. When the gas passing through the point B_1 reaches the position x_2, the other arrives at the point A_2 because the velocity in the boundary layer is larger than that in the free-stream. The temperature at A_3 is lower than that at A_2. Therefore, the temperature of the gas at B_2 is higher than that at A_3, if all the effects of the boundary layer can be dismissed except the effect of the velocity. The discussion above may be the main reason for the temperature overshoot, in spite of the fact that in the boundary layer, thermal conduction occurs, and that the ionization and the energy transfer are different from that of free-stream.

Fig. 7 shows the temperature profiles of the electron gas in the boundary layer. The electron temperature profile does not vary until the free-stream becomes equilibrium. The electron temperature near the wall, in the equilibrium region of the free-stream, decreases towards downstream. This results from the energy transfer due to elastic collisions and ionization reacting near the wall.

Fig. 8 shows the profiles of degree of ionization in the boundary layer. The

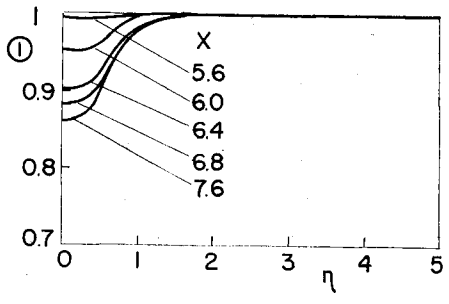

Fig. 7. Electron temperature profiles in the boundary layer.

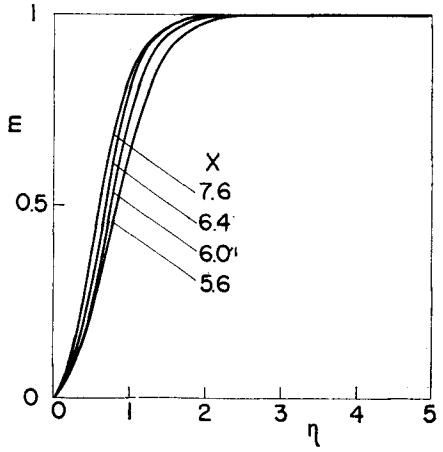

Fig. 8. Profiles of degree of ionization in the boundary layer.

distribution of the ionization degree does not change essentially until the free-stream becomes equilibrium. After the equilibration of the free-stream, the degree of ionization begins to increase as the ionization proceeds in the boundary layer. This is because the degree of ionization is small near the wall and the electron temperature is still high enough to ionize.

The gradients of the heavy particle temperature $\theta_{\eta w}$ and non-dimensional ion current $M_{\eta w}$ have been obtained with the accuracy of $O(h^2)$ by using an extrapolation formula.

Fig. 9 shows $N_u/\sqrt{R_x}$. Nusselt number N_u and Reynolds number R_x are defined as follows

$$N_u = \frac{lx}{T_\delta - T_w}\frac{\partial T}{\partial y}\bigg|_w \tag{42}$$

$$R_x = (\rho_0 u_0 l x)/\mu_0 \tag{43}$$

where x is in a non-dimensional scale and l is the unit length.

Fig. 10 shows the ion current defined as follows:

$$I = \frac{e}{m_a}\rho D_a \frac{\partial}{\partial y}\left(C\frac{1+T_e/T}{2}\right)\bigg|_w \tag{44}$$

where e is the electron charge. The coordinate of t in Fig. 10 is the time elapsed after the shock arriving at the observing point. In the present analysis, the side

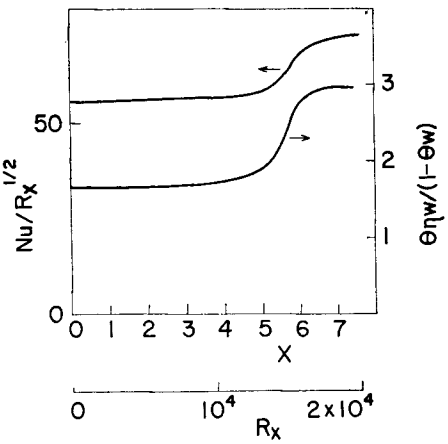

Fig. 9. Variation of Nusselt number in the region behind a shock wave.

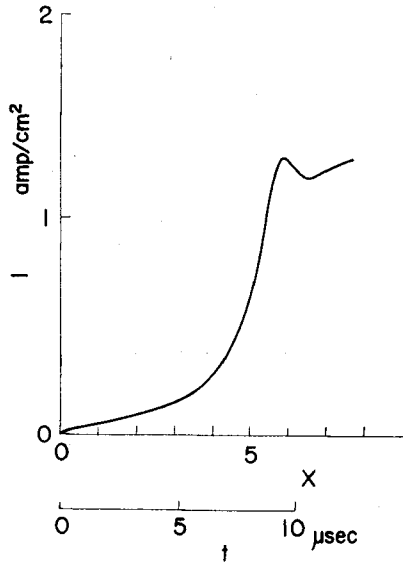

Fig. 10. Variation of the ion current after a shock arrival.

wall is assumed to be at a floating potential. Therefore, the net current flowing to the wall is zero. However, the ion saturation current of an electrostatic probe seems to be this ion current itself, because the ion currents are not so much influenced by a wall potential as are the electron currents.

7. Conclution

The numerical analysis was made for an ionizing and thermally non-equilibrium boundary layer over a shock-tube side-wall. It was found that the temperature in the boundary layer is higher than that outside of the boundary layer in the rapidly ionizing region of the free-stream. The profiles of electron temperature and degree of ionization were found to vary according to the change of the free-stream. In the present analysis, several assumptions were made and the analysis of rigorous equations must be made hereafter.

Appendix

Boundary Conditions with a Free Fall Sheath

When the wall is at floating potential, the boundary conditions[2),4)] at the wall for number density and temperature of the electron gas are

$$\left[\rho D_a \frac{\partial}{\partial y}\left(C\frac{1+T_e/T}{2}\right)\right]_s = \rho_s C_s \left(\frac{kT_{es}}{m_a}\right)^{1/2} \tag{A-1}$$

$$\left[\lambda_e \frac{\partial T_e}{\partial y}\right]_s = \left(-\frac{1}{2}R_A T_{es} + \frac{e\Delta\phi}{m_a}\right)\rho_s C_s \left(\frac{kT_{es}}{m_a}\right)^{1/2} \tag{A-2}$$

where s refers to the sheath edge and $\Delta\phi$ means the potential difference between a wall and a sheath edge. The conditions for nondimensional equations are

$$[M_\eta]_w = S_c \frac{\sqrt{2\xi}}{\mu_\delta}\frac{V_{i\delta}}{u_\delta}\frac{m_w}{\theta_w}\Theta_w^{1/2} \tag{A-3}$$

$$[\Theta_\eta]_w = \frac{2}{5}\frac{P_{re}}{S_c}\left(-\frac{1}{2}\Theta_w + \frac{e\Delta\phi}{kT_{es}}\right)\frac{\theta_w}{\Theta_w^{5/2}}[M_\eta]_w \tag{A-4}$$

where $V_{i\delta}=(kT_{es}/m_a)^{1/2}$

In the present calculation, we use the values as follows

$$P_{re} = 0.0179\,,\quad S_c = 2.3\,,\quad \theta_w < 0.02$$
$$M_{\eta w} = 0.5\sim 0.7\,,\quad \Theta_w = 0.8\sim 1\,,\quad e\Delta\phi/kT_{es} = 0(1)$$

With the relation of $\sqrt{2\xi}/\mu_\delta \simeq \sqrt{2R_x}$, equations (A-3) and (A-4) yield

$$\Theta_{\eta w} = 0(10^{-4})$$
$$m_w = 0(10^{-2})/\sqrt{R_x}$$

When $x \geq 1$, $m_w = 0$ can be used because $R_x = 0.265 \times 10^4$ at $x = 1$ of the non-dimensional axis. $\theta_{\eta w} = 0$ can be used unless θ_w decreases considerably.

References

1) Knöös, S.: Boundary-Layer Structure in a Shock-Generated Plasma Flow, Part 1. Analysis for Equilibrium Ionization. J. Plasma Phys., Vol. 2, 1968.
2) Honma, H. and Aoki, I.: Ionized Nonequilibrium, Laminar Boundary Layer behind a Moving Shock Wave (1) Local Similar Analysis for Quasi-equilibrium Flow, J. Faculty of Engineering, Chiba Univ. (to be published)
3) Tseng, R.C. and Talbot, L.: Flat Plate Boundary Layer in a Partially Ionized Gas. AIAA J., Vol. 9, No. 7, 1971.
4) Nishida, M. and Matsuoka, K.: Structure of Nonequilibrium Boundary Layer along a Flat Plate in a Partially Ionized Gas. AIAA J. Vol.9 No.11, 1971, Author Rep. No. 70-1 (NTC-45-6).
5) Blottner, F.G.: Finite Difference Methods of Solution of the Boundary-Layer Equations. AIAA J., Vol.8, No. 2, 1970.
6) Chung, P.M., Talbot, L. and Touryan, K.J.: Electric Probes in Stationary and Flowing Plasmas: Part 1. Collisionless and Transitional Probes, and Part 2. Continuum Probes. AIAA J., Vol. 12, No. 2, 1974.
7) Hoffert, M.I. and Lien, H.: Quasi-One-Dimensional Nonequilibrium Gas Dynamics of Partially Ionized Two-Temperature Argon. Phys. Fluid., Vol. 10, No. 8, 1967.
8) Wong, H. and Bershader, D.: Thermal Equilibration behind an Ionizing Shock.: J. Fluid Mech., Vol. 10, No. 8, 1966.
9) Chung, P.M. and Mullen, J.F.: Nonequilibrium Electron Temperature Effects in Weakly Ionized Stagnation Boundary Layer. AIAA Paper, No. 63-161 Los Angeles, Calif., June 1963.
10) Chung, P.M.: Chemical Reacting Nonequilibrium Boundary Layer. Heat Transfer, Vol. 2, 1964.